# SIMULATION AND DYNAMICAL CHARACTERIZATION OF AN ACTIVE MECHANICAL CHAOTIC DOUBLE PENDULUM

**Davidson Lafitte Firmo, lafitte@cpdee.ufmg.br**
**Leonardo A. B. Tôrres, torres@cpdee.ufmg.br**
Universidade Federal de Minas Gerais – UFMG. Av. Antônio Carlos, 6627 – Pampulha – Belo Horizonte – MG – Brazil

**Erivelton G. Nepomuceno, nepomuceno@ufsj.edu.br**
Universidade Federal de São João del-Rei – UFSJ. Pça. Frei Orlando, 170 – Centro – São João del-Rei – MG – Brazil

***Abstract.*** *The aim of the present work is the design of a low cost autonomous chaotic oscillator that could be used seamlessly for research or in class demonstrations. At the same time, one should be able to easily reproduce the final system in other educational institutions. Based on these requirements, a chaotic electromechanical oscillator is proposed. The system is comprised by a mechanical double pendulum, a DC motor driver, and the accompanying signal processing electronic circuits, together with an appropriate speed feedback arrangement that guarantees the existence of sustained mechanical oscillations. In this paper, the oscillator mathematical model and its dynamical characterization from simulated time-series analysis are presented. The chaotic nature of the system for different parameters, such as viscous friction coefficients, is investigated through the estimation of the associated largest positive Lyapunov exponent.*

***Keywords:*** *double pendulum, dynamic characterization, chaos, time series analysis*

## 1 INTRODUCTION

In the recent times, chaos theory has become widespread in the scientific literature, and more recently it has entered the engineering domain through the use of chaotic oscillators based systems and methods in many diverse areas (Tôrres and Aguirre, 2004; Marinho et al., 2005; Goldberger, 1990; Andrievskii and Fradkov, 2004). Indeed, in these times such knowledge could be regarded as essential to the completion of a well thought engineering education.

In this context, the proposition of easily reproducible and visually appealing experimental apparatus focused on the introduction of engineering students into the chaos theory world is most welcome. Clearly, such experimental platforms can also serve as supporting material in nonlinear dynamics introductory courses. Moreover, one expects that sound research can be initiated based on well designed experiments (Berger and Nunes, 1997; Blackburn and Baker, 1998; Chua et al., 1993; Laws, 2004; Shinbrot et al., 1991; Tôrres and Aguirre, 2005).

This is particularly true in the case of pendulum based systems. There is an expressive amount of traditional physical knowledge related to observed phenomena in pendula, from Galileo-Galilei and the famous observation of a pendulum in periodic motion in the cathedral of Pisa, through other examples found in recent literature (Fiedler-Ferrara and Prado, 1994; Monteiro, 2002). As shown in several works (Shinbrot et al., 1991; Christini et al., 1996; Zhou and Whiteman, 1996; Skeldon, 1994) for double pendulum, and in (Smith and Blackburn, 1989; Blackburn and Baker, 1998; Franca and Savi, 2001; Laws, 2004) for simple pendulum, such systems can exhibit chaotic behavior if properly designed.

On the other hand, despite the existence of comercial experimental platforms that could be employed to demonstrate chaotic dynamics to engineering students, the cost of a comercial system is usually in the ranges from US$1,200 up to US$2,000 (Blackburn and Baker, 1998), which is considered high cost in many brazilian educational institutions. At the same time, the reproduction of such comercial systems, by using local material and labor, is not possible due to the violation of copyright laws.

Another interesting point is that it seems to lack, on the present literature, a description of a double pendulum based system which is autonomous. These systems are usually excited by periodic external functions.

The main objective of the present paper is to present an *autonomous electromechanical double pendulum experimental platform,* for educational and research purposes, whose cost is kept as low as possible such that the reproduction of the proposed experimental system by other educational institutions in Brazil becomes feasible. Based on its mathematical model, obtained from first principles, simulation results will be presented together with the dynamical characterization of the system through the estimation of the largest Lyapunov exponent.

The paper is organized as follows. In Section 2, a brief historical accounting of pendulum based systems is done and the proposed experimental platform is presented in Sections 2.1 and 2.2. In Section 2.3 a mathematical model is derived from first principles, including friction effects to model the damping in the system. Simulation results are presented in Section 3, where dynamical analysis is conducted to estimate the system largest Lyapunov exponent. Finally, in Section 4 conclusions related to the dynamical characterization of the system and to its cost are presented.

## 2 AN ACTIVE DOUBLE PENDULUM

Many works can be found on the scientific literature related to the modelling and simulation of pendulum based systems (Skeldon, 1994; Levien and Tan, 1993; Zhou and Whiteman, 1996). Real results were also reported in (Shinbrot et al., 1991; Christini et al., 1996). Despite this, information on the use of double pendulum for educational purposes seems to be restricted to passive (non-excited) versions, as presented in Shinbrot et al. (1991).

A key observation is that even the passive double pendulum system exhibits sensitivity to initial conditions (Shinbrot et al., 1991). However, in the absence of excitation, the system tends to stop due to the energy lost to overcome friction forces. Therefore, chaotic behavior is not possible in this case, once the required transitivity property cannot be verified, which violates the definition of chaos according to Devaney (1992).

In order to design a mechanical apparatus capable of exhibiting sustained oscillations, it is necessary to continuosly provide energy to the system. As it will be shown in the next section, this is accomplished in the proposed platform in such a way that the overall system remains autonomous.

### 2.1 General Description

The proposed experimental system is presented in Fig.1a. The apparatus is comprised by two bars linked to form a double pendulum. A DC motor drive is used to supply energy to the system by applying torque on the first bar; which rotates together with the rotor of the DC motor. The angular position of the bars in the double pendulum are denoted by $\theta_1$ and $\theta_2$, as shown in Fig.1, with corresponding angular speeds $\dot{\theta}_1$ and $\dot{\theta}_2$. The torque applied by the DC motor drive is a function of $\theta_1$ and $\dot{\theta}_1$, denoted by $G(\theta_1, \dot{\theta}_1)$ in the figure, such that the overall system remains autonomous; i.e. no external excitation explicitly dependent on time is applied, as it would be the case, for example, if a periodic forcing function was employed. In Fig.1b a signal flow diagram is depicted showing how bar 1 position and speed signals are fed back into the system.

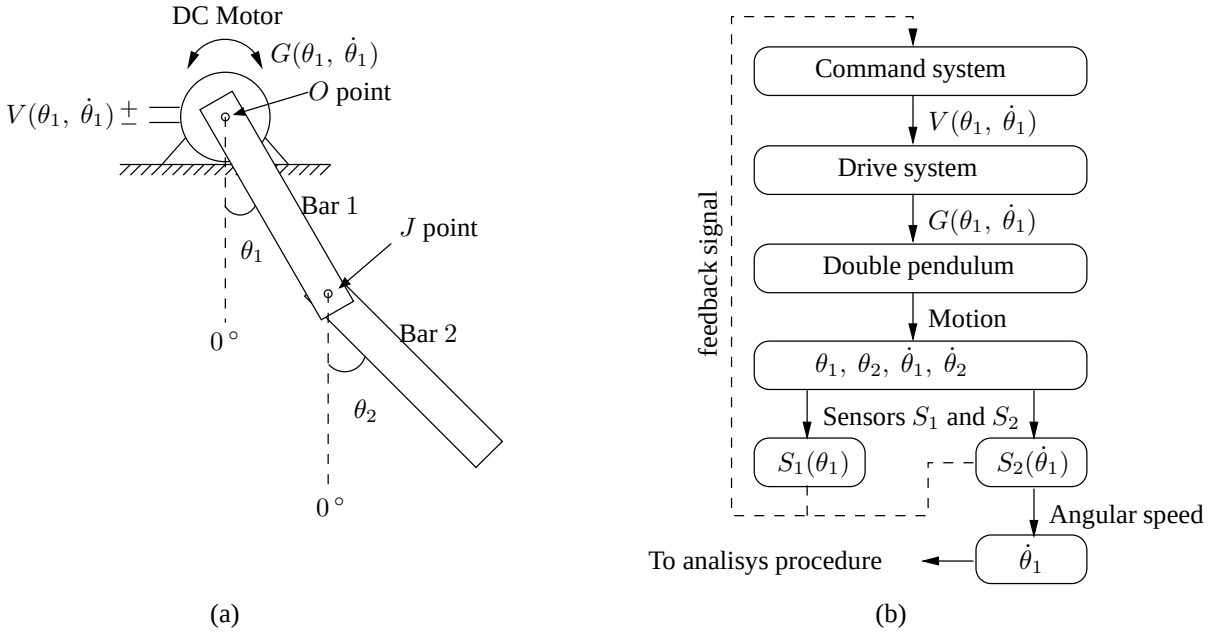


Figure 1. (a) Proposed apparatus – a double pendulum connected to a DC motor drive. (b) Signal flow block diagram.

The command subsystem block, shown in Fig.1b, generates full or zero DC voltage commands to the motor drive subsystem, based on the signals provided by the sensors $S_1$ and $S_2$. An issued full DC voltage command is such that it has always the same sign of $\dot{\theta}_1$. In this way, the motor drive torque always act in the same instantaneous direction of rotation of bar 1. However, this only occurs when $|\theta_1| < \gamma$, where $\gamma$ is a limit angle. If $|\theta_1| \geq \gamma$, a zero DC voltage command is sent to the DC motor drive subsystem, and it becomes a short-circuited DC generator.

The motor drive subsystem is comprised by an electrical universal motor; taken from a domestic AC sewing machine, and adapted to work as a DC motor by properly exciting its field winding. An H-bridge electronic circuit is used to reverse the polarity of the full DC voltage applied to the motor drive armature coil, and also to short-circuit the motor terminals when $|\theta_1| \geq \gamma$. In both cases, the circulation of an instantaneous armature current $i_a$ is allowed.

The sensor $S_1$ is implemented by using an infrared light emitting diode – LED and phototransistor matched pair, together with a small transparent plastic disc painted such that a high logic level is produced only when $|\theta_1| < \gamma$. Sensor $S_2$ is a tiny DC motor bonded to the DC motor drive axis, acting as a DC generator, such that a signal proportional to $\dot{\theta}_1$

is produced. The output signals from sensors $S_1$ and $S_2$ are such that they can be modelled by the following expressions:

$$S_1(\theta_1) = \begin{cases} 0, \text{ if } & |\theta_1| \geq \gamma; \\ 1, \text{ if } & |\theta_1| < \gamma; \end{cases} \qquad S_2(\dot{\theta}_1) = k_\omega \dot{\theta}_1; \tag{1}$$

where $k_\omega \in \mathbb{R}^+$ is a constant.

The operation of the motor drive subsystem can be summarized as shown in Table 1, which reveals that this subsystem is designed to provide energy to the double pendulum whenever $|\theta_1| < \gamma$.

Table 1. *Motor drive operation.*

| Sensors Outputs | | Motor States |
|---|---|---|
| $S_1(\theta_1)$ | $S_2(\dot{\theta}_1)$ | |
| 1 | $> 0$ | Driven to rotate in the clockwise direction. |
| 1 | $< 0$ | Driven to rotate in the counterclockwise direction. |
| $S_1(\theta_1) = 0$ | | Short-circuited DC generator. |

### 2.2 Mechanical Apparatus

The mechanical design of the proposed system follows closely the work presented by Shinbrot et al. (1991). However, small modifications were added to adequately incorporate the excitation from the DC motor drive.

The bar 1 in the double pendulum is actually formed by two aluminum rectangular pieces, with dimensions $0.27\text{m} \times 0.032\text{m} \times 0.006\text{m}$, and total mass (bar 1) $m_1 = 0.152\text{kg}$, joined so that double pendulum bar 2 can execute a complete revolution, as shown in Fig.2. The interconnection between bars 1 and 2 is done using a steel axis, located in the $J$ point shown in Fig.1a.

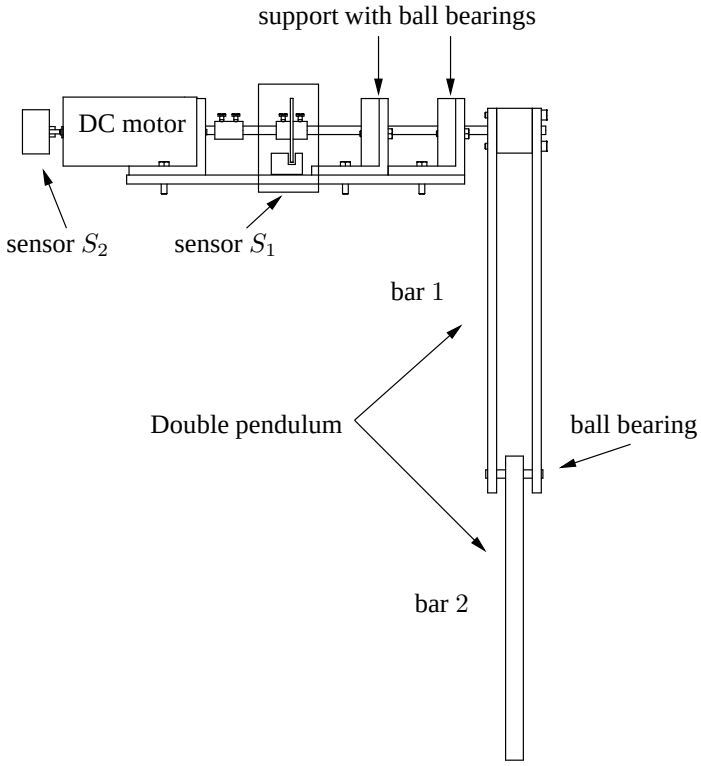


Figure 2. Proposed apparatus – lateral view.

Bar 2 is also a retangular aluminum piece, with dimensions $0.216\text{m} \times 0.032\text{m} \times 0.013\text{m}$, fixed to the middle point of the aforementioned steel axis. The axis is supported by two ball bearings, each one fixed at one of the aluminum pieces that comprise bar 1 (Fig.2). In this way, bar 2 can rotate freely around the $J$ point, while bar 1 rotates around the $O$ point, as shown in Fig.1a, fixed to the DC motor drive axis.

The mechanical system inertia can be computed from the dimensions of bars 1 and 2 together with the density $\rho$ of the aluminum material employed in the pendulum construction ($\rho = 2,700\text{kg/m}^3$). The motor inertia $M_m$ is computed separately by performing independent experiments, and it was found to be $M_m = 22 \times 10^{-6}\text{kg.m}^2$.

The DC motor drive axis is extended by the connection to a stainless steel round rod that goes through two supporting ball bearings, which are fixed at aluminum blocks attached to a base made of steel (Fig.2). The plastic disc of sensor $S_1$ is fixed to this rod.

The total friction in the system can be accounted for by considering the viscous friction in all the supporting ball bearings mentioned above, together with the viscous friction in the bearings used in the DC motor drive construction, and the air resistance to the movements of bars 1 and 2. The moment produced by these viscous friction forces are considered to be proportional to instantaneous angular speed. Despite of being constants, the opposing friction forces (Coulomb friction) at the DC motor drive bearings and at all the other ball bearings are also taken into account.

All the friction forces are considered to be applied at points $O$ and $J$ in Fig.1a. At the point $O$, the total viscous friction coefficient is denoted by $b_{m1}$, and the Coulomb friction is represented by $b_{m2}$. At the point $J$, the total viscous friction coefficient is denoted by $b_3$, and the Coulomb friction is represented by $b_4$.

### 2.3 Mathematical Equations

The point of origin of an inertial reference frame is defined to be the $O$ point in Fig.1a. The equations of motion can be derived from the application of Steiner's theorem and Newton laws at each center of mass – c.m. of each bar, such that:

$$\sum F_x = ma_{c,x}, \qquad \sum F_y = ma_{c,y}, \qquad \sum M_O = I_O\ddot{\theta}, \tag{2}$$

where $\sum F_x$ is the total force acting in the $x$ direction; $\sum F_y$ is the total force acting in the $y$ direction; $a_{c,x}$ and $a_{c,y}$ are the horizontal and vertical accelerations of the c.m. of each bar relative to the inertial reference frame; $M_O$ is the total moment around the $O$ point for a specific bar; $I_O$ is the bar moment of inertia around $O$; and $\ddot{\theta}$ is the corresponding angular acceleration.

Let $m_1$ and $m_2$ be the masses of bars 1 and 2, respectively, and $l_1$ and $l_2$ its corresponding lengths.

The forces acting on the systems are the bars weights $m_1 g$ and $m_2 g$; where $g$ is the acceleration of gravity ($g = 9.8\text{m/s}^2$); the torque $G(\theta_1, \dot{\theta}_1)$ applied by the DC motor drive, the viscous and Coulomb friction forces on bar 1, denoted by $b_{m1}\dot{\theta}_1 + b_{m2}\,\text{sgn}(\dot{\theta}_1)$, and the corresponding viscous and Coulomb friction forces on bar 2, denoted by $b_3(\dot{\theta}_2 - \dot{\theta}_1) + b_4\,\text{sgn}(\dot{\theta}_2 - \dot{\theta}_1)$. There are also internal forces $J_x$ and $J_y$ that keep the bars connected. Free-body diagrams, for each bar, are depicted in Fig.3.

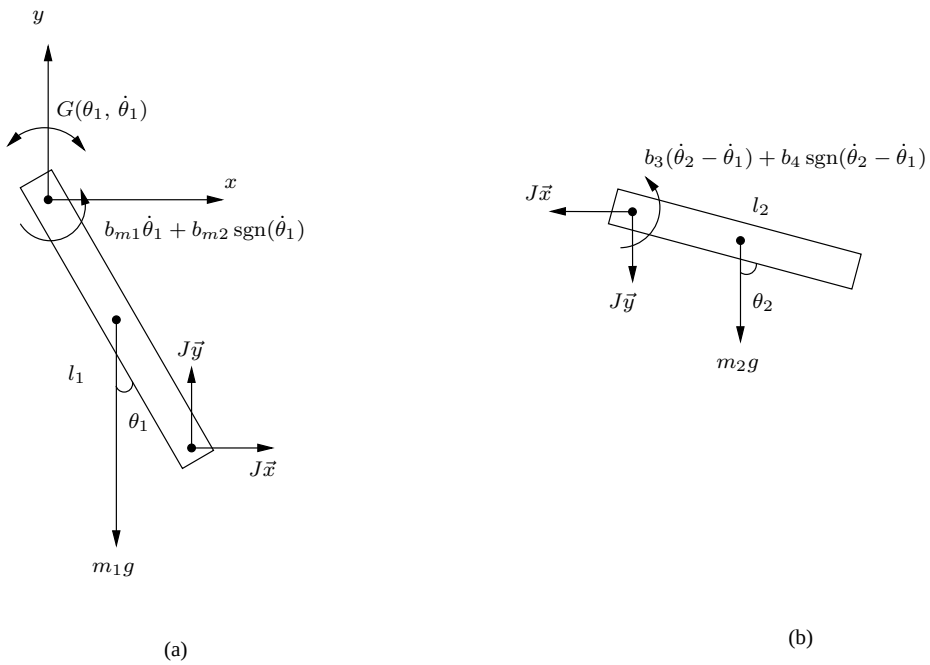


Figure 3. Double pendulum free-body diagrams. (a) Bar 1 and (b) bar 2.

By applying equations (2) to the free-body diagrams shown in Fig.3, one has that, for bar 1:

$$-m_1\, g\, \frac{l_1\, sen(\theta_1)}{2} + J_y\, l_1\, sen(\theta_1) + J_x\, l_1\, cos(\theta_1) - b_{m1}\, \dot{\theta}_1 - b_{m2}\, \text{sgn}(\dot{\theta}_1) + G(\theta_1, \dot{\theta}_1) = \left(\frac{1}{3}\, m_1\, l_1^2 + M_m\right) \ddot{\theta}_1, \tag{3}$$

and, for bar 2,

$$J_x \frac{l_2\, cos(\theta_2)}{2} + J_y \frac{l_2\, sen(\theta_2)}{2} - b_3\,(\dot{\theta}_2 - \dot{\theta}_1) - b_4\ \mathrm{sgn}(\dot{\theta}_2 - \dot{\theta}_1) = \frac{1}{12}\, m_2\, l_2^2\, \ddot{\theta}_2. \tag{4}$$

The internal forces $J_x$ and $J_y$, acting at the $J$ point, are related by

$$J_x = -m_2\, a_{C_2,x} \qquad\qquad J_y = -m_2\, a_{C_2,y} - m_2\, g,$$

where $a_{C_2,x}$ and $a_{C_2,y}$ are the horizontal and vertical acceleration of the bar 2 c.m.. The acceleration $a_{C_2}$ is the sum of the $J$ point acceleration $a_J$, with the relative acceleration $a_{C_2/J}$ of the bar 2 c.m. relative to the $J$ point: $a_{C_2} = a_J + a_{C_2/J}$. The acceleration $a_{C_2}$ can be determined based on the concept of relative movement (Meriam and Kraige, 2003), such that

$$\vec{a}_{C_2} = \vec{\ddot{\theta}}_1 \times \vec{r}_{J/O} + \vec{\dot{\theta}}_1 \times (\vec{\dot{\theta}}_1 \times \vec{r}_{J/O}) + \vec{\ddot{\theta}}_2 \times \vec{r}_{C_2/J} + \vec{\dot{\theta}}_2 \times (\vec{\dot{\theta}}_2 \times \vec{r}_{C_2/J}) \tag{5}$$

where $\vec{r}_{J/O} = l_1\,(sen(\theta_1)\,\vec{i} - cos(\theta_1)\,\vec{j})$, and $\vec{r}_{C_2/J} = \frac{l_2}{2}\,(sen(\theta_2)\,\vec{i} + cos(\theta_2)\,\vec{j})$.

To find the equations for $\ddot{\theta}_1$ and $\ddot{\theta}_2$ it is necessary to consider the torque, $G(\theta_1,\, \dot{\theta}_1)$, as a function of the DC motor drive armature current, $i_a$, such that:

$$G(\theta_1,\, \dot{\theta}_1) = K_t\, i_a(\theta_1,\, \dot{\theta}_1), \tag{6}$$

$$\dot{i}_a = \frac{V(\theta_1,\, \dot{\theta}_1) - K_s\, \dot{\theta}_1 - R_a\, i_a}{L_a}, \tag{7}$$

where $K_t$, $K_s$, $R_a$ and $L_a$ are DC motor drive constructive parameters, and $V(\theta_1,\, \dot{\theta}_1)$ is the voltage applied to armature coil.

From the above relations, and back substitution into equations 3 and 4, it is possible to isolate the following equations for $\ddot{\theta}_1$ and $\ddot{\theta}_2$:

$$\ddot{\theta}_1 = \left( \frac{-3\, g\, l_1\, sin(\theta_1)\,(4\, m_1 + 5\, m_2) + 9\, m_2\, l_1\,(g\, sin(-\theta_1 + 2\,\theta_2) + l_1\, \dot{\theta}_1^2\, sin(2\,\beta)) + 12\, m_2\, l_1\, l_2\, \dot{\theta}_2^2\, sin(\beta)}{8\, M_m + 8\, m_1\, l_1^2 + 15\, m_2\, l_1^2 - 9\, m_2\, l_1^2\, cos(2\,\beta)} + \right.$$
$$\left. \frac{36\, l_1\, cos(\beta)\,(b_4\ \mathrm{sgn}(\dot{\beta}) + b_{m2}\, \dot{\beta}) - 24\, l_2\,(\, b_{m1}\, \dot{\theta}_1 \,-\, K_t\, i_a(\theta_1,\, \dot{\theta}_1) \,+ b_{m2}\ \mathrm{sgn}(\dot{\theta}_1)\,))}{l_2\,(8\, M_m + 8\, m_1\, l_1^2 + 15\, m_2\, l_1^2 - 9\, m_2\, l_1^2\, cos(2\,\beta))} \right), \tag{8}$$

$$\ddot{\theta}_2 = \left( \frac{-24\,(b_{m2}\, \dot{\beta}\,(M_m + m_1\, l_1^2 + 3\, m_2\, l_1^2) + b_4\ \mathrm{sgn}(\dot{\beta})\,(M_m + m_1\, l_1^2 + 3\, m_2\, l_1^2))}{m_2\, l_2^2\,(8\, M_m + 8\, m_1\, l_1^2 + 15\, m_2\, l_1^2 - 9\, m_2\, l_1^2\, cos(2\,\beta))} + \right.$$
$$\frac{-12\, l_1\, \dot{\theta}_1^2\, sin(\beta)\,(M_m + m_1\, l_1^2 + 3\, m_2\, l_1^2) - 9\, l_1^2\, g\, sin(-2\,\theta_1 + \theta_2)\,(m_1 + 2\, m_2)}{l_2\,(8\, M_m + 8\, m_1\, l_1^2 + 15\, m_2\, l_1^2 - 9\, m_2\, l_1^2\, cos(2\,\beta))} +$$
$$\frac{-36\, l_1\, cos(\beta)\, K_t\, i_a(\theta_1,\, \dot{\theta}_1) - b_{m1}\, \dot{\theta}_1 - b_{m2}\ \mathrm{sgn}(\dot{\theta}_1)) - 3\, sin(\theta_2)\, g\,(m_1\, l_1^2 + 6\, m_2\, l_1^2 + 4\, M_m)}{l_2\,(8\, M_m + 8\, m_1\, l_1^2 + 15\, m_2\, l_1^2 - 9\, m_2\, l_1^2\, cos(2\,\beta))} +$$
$$\left. \frac{-9\, m_2\, l_1^2\, \dot{\theta}_2^2\, sin(2\,\beta)}{8\, M_m + 8\, m_1\, l_1^2 + 15\, m_2\, l_1^2 - 9\, m_2\, l_1^2\, cos(2\,\beta)} \right), \tag{9}$$

$$\dot{i}_a = \left( \frac{V(\theta_1,\, \dot{\theta}_1) - K_s\, \dot{\theta}_1 - R_a\, i_a}{L_a} \right). \tag{10}$$

Where $\beta = \theta_2 - \theta_1$ and $\dot{\beta} = \dot{\theta}_2 - \dot{\theta}_1$.

## 3 SIMULATION RESULTS AND TIME SERIES ANALYSIS

The model was simulated using a fourth order Runge-Kutta method. It has been used different values for damping coefficients. A time series of angular speed $\dot{\theta}_1$ of bar 1 was used to estimate the greatest Lyapunov exponent for each case. Table 2 shows the damping coefficients used for simulations, the other parameters are shown in Table 3.

Table 2. *Damping coefficients values used in each simulation.*

| Parameters | | | | | Simulation |
|---|---|---|---|---|---|
| $b_{m1}$ | $b_{m2}$ | $b_3$ | $b_4$ | Voltage applied to motor† | |
| 0.0010 | 0.0010 | 0.000015 | 0.00015 | $30V$ | 1 |
| 0.0014 | 0.0014 | 0.000017 | 0.00017 | $30V$ | 2 |
| 0.0025 | 0.0025 | 0.000019 | 0.00019 | $30V$ | 3 |

† Applicable maximum voltage regarding to current limits.

Table 3. *Parameters and values used in simulations.*

| Parameters | $k_s$ | $k_t$ | $\gamma$ | $R_a$ | $L_a$ | $l_1$ | $l_2$ | $m_1$ | $m_2$ | $M_m$ |
|---|---|---|---|---|---|---|---|---|---|---|
| Values | 0.0358 | 0.0358 | 1.05 | 32 | 0.03 | 0.273 | 0.216 | 0.297 | 0.236 | $22 \cdot 10^{-6}$ |
| Units | $--$ | $--$ | rad | $\Omega$ | H | m | m | kg | kg | $\mathrm{kg.m}^2$ |

The values of constants used in the simulation procedure are shown in Table 3. For the reconstruction of the phase space, it has been used the mutual information method to specify a suitable delay. The immersion dimension was calculated by means of false neighbors and Lyapunov exponent was determined by the algorithm proposed by Kantz (1994). All algorithms have been implemented in the TISEAN toolbox (Hegger et al., 1999). The results are shown in Table 4.

Lyapunov exponents were estimated using the immersion dimensions 5, 6 and 7. An average of the three values was obtained with the corresponding sample variance. In the simulations 1 and 2 the Lyapunov exponents were positive, which may indicate a chaotic regime. For simulation 3, the results show that the trajectory is not convergent and neither divergent, that is, the Lyapunov exponent is null and the regime is periodic. Figure 4 shows the phase space of $\theta_1$ and $\dot{\theta}_1$ for each case.

Figures 4a and 4b show a projection over the strange atractor of the system. Figure 4c shows periodic behavior observed in simulation 3.

## 4 CONCLUSIONS

In this paper, the design and dynamical characterization of an active double pendulum electromechanical system was presented. From the perspective of a low cost based system, the system proposed was designed using a DC motor, a mechanical pendulum and an electronic apparatus to guarantee a sustained mechanical oscillations.

It is possible to summarize the following points. Firstly, regarding the damping, there is a limit above which the system exhibits only periodic motion, and the sensitivity to initial conditions is lost. However, this problem can be avoided by using a more powerful dc motor.

The results obtained by working with chaotic time series must be used with care, because the mathematical procedure to find the greatest Lyapunov exponent assumes an infinite time series, which is unfeasible in both numerical simulations and in experiments. The results from the analysis indicate a positive Lyapunov exponent, thus the existence of a chaotic regime.

The proposed experimental system is being developed at Universidade Federal de Minas Gerais and the cost of a first prototype is approximately US$ 200.00.

By the time of the end of the present paper revision process, preliminary practical results were obtained and the corresponding dynamical characterizarion is being performed. These real results will be submitted to publication in a near future.

Table 4. *Analysis of the simulated time series ($\dot{\theta}_1$), and used parameters to reconstruct the phase space.*

| Simulation | Delay (Mutual Information) | Dimension (False neighbors) | Lyapunov Exponent: $\lambda_1$ |
|---|---|---|---|
| 1 | 36 | $5\,(0.4\%),\ 7\,(0.02\%)$ | $1.39 \pm 0.25$ |
| 2 | 35 | $5\,(0.4\%),\ 7\,(0.06\%)$ | $1.24 \pm 0.17$ |
| 3 | 8 | 1 | $0^{\ddagger}$ |

‡ Expected values for periodic systems.

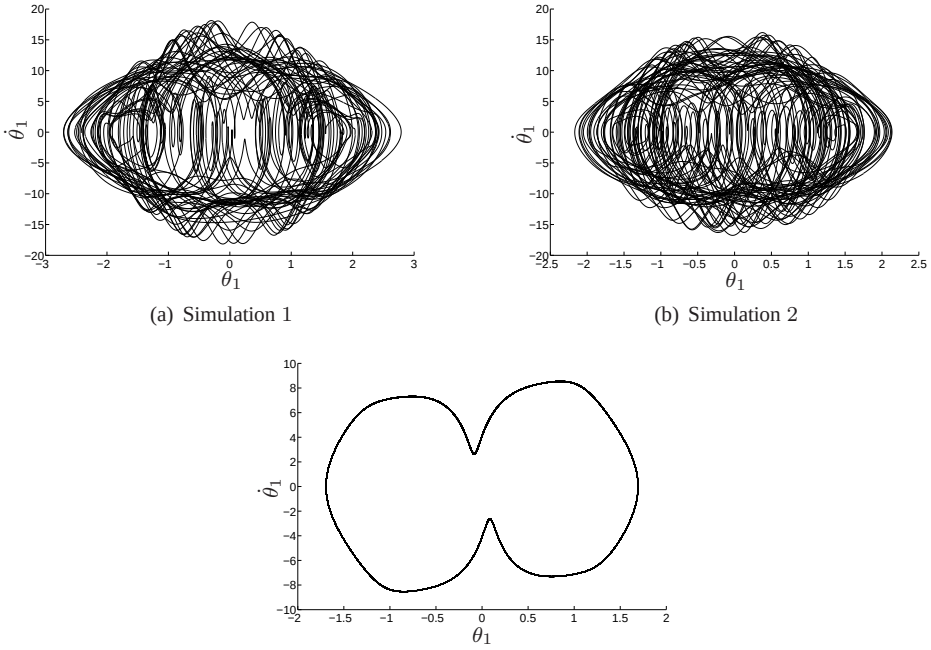


(a) Simulation 1

(b) Simulation 2

(c) Simulation 3

Figure 4. Phase portrait of the proposed systems - The greatest Lyapunov exponent ($\lambda_1$): (a) $\lambda_1 = 1.39 \pm 0.25$; (b) $\lambda_1 = 1.24 \pm 0.17$; (c) $\lambda_1 = 0$

## 5 REFERENCES

Andrievskii, B. R. and Fradkov, A. L., 2004. "Control of Chaos: Methods and Applications. II. applications". Automation and Remote Control, vol. 65, no. 4, pp. 505–533.

Berger, J. E. and Nunes, G., 1997. "A Mechanical Duffing Oscillator for the Undergraduate Laboratory". American Journal of Physics, vol. 65, no. 9, pp. 841–846.

Blackburn, J. A. and Baker, G. L., 1998. "A Comparison of Commercial Chaotic Pendulums". American Journal of Physics, vol. 66, no. 9, pp. 821–830.

Christini, D. J., Collins, J. J. and Linsay, P. S., 1996. "Experimental control of high-dimensional chaos: The driven double pendulum". Physical Review E, vol. 54, no. 5, pp. 4824–4827.

Chua, L. O., Wu, C. W., Huang, A. S. and Zhong, G. Q., 1993. "A Universal Circuit for Studying and Generating Chaos. 1 Routes to Chaos". IEEE Transactions on Circuits and Systems, vol. 40, no. 10, pp. 732–744.

Devaney, R. L., 1992. A First Course in Chaotic Dynamical Systems: Theory and Experiment. Reading.

Fiedler-Ferrara, N. and Prado, C. P. C., 1994. Caos uma Introdução. Editora Edgard Blücher Ltda.

Franca, L. F. and Savi, M. A., 2001. "Distinguishing Periodic and Chaotic Time Series Obtained from an Experimental Nonlinear Pendulum". Nonlinear Dynamics, vol. 26, no. 3, pp. 253–271.

Goldberger, A. L., 1990. "Nonlinear Dynamics, Fractals and Chaos: Applications to Cardiac Electrophysiology". Annals of Biomedical Engineering, vol. 18, no. 2, pp. 195–198.

Hegger, R., Kantz, H. and Schreiber, T., 1999. "Practical Implementation of Nonlinear Time Series Methods: The Tisean Package". Chaos, vol. 9, no. 413.

Kantz, H., 1994. "A Robust Method to Estimate the Maximal Lyapunov Exponent of a Time Series". Physics Letters A, vol. 185, no. 1, pp. 77–87.

Laws, P. W., 2004. "A Unit on Oscillations, Determinism and Chaos for Introductory Physics Students". American Journal of Physics, vol. 72, no. 4, pp. 446–452.

Levien, R. B. and Tan, S. M., 1993. "Double pendulum: An experiment in chaos". American Jounal of Physics, vol. 61, no. 11, pp. 1038–1044.

Marinho, C. M. P., Macau, E. E. N. and Yoneyama, T., 2005. "Chaos Over Chaos: A New Approach for Satellite Communication". Acta Astronautica, vol. 57, no. 2-8, pp. 230–238.

Meriam, J. L. and Kraige, L. G., 2003. Engineering Mechanics. John Wiley & Sons, Inc.

Monteiro, L. H. A., 2002. Sistemas Dinâmicos. Editora Livraria da Física.

Shinbrot, T., Grebogi, C., Wisdom, J. and Yorke, J. A., 1991. "Chaos in a double pendulum". American Journal of Physics, vol. 60, no. 6, pp. 491–499.

Skeldon, A. C., 1994. "Dynamics of a parametrically excited double pendulum". Physica D, vol. 75, pp. 541–558.

Smith, H. J. T. and Blackburn, J. A., 1989. "Chaos in a Parametrically Damped Pendulum". Physical Review A, vol. 40, no. 8, pp. 4708–4715.

Tôrres, L. A. B. and Aguirre, L. A., 2004. "Transmitting Information by Controlling Nonlinear Oscillators". Physica D, vol. 196, no. 3-4, pp. 387–406.

Tôrres, L. A. B. and Aguirre, L. A., 2005. "PCCHUA - A Laboratory Setup for Real-Time control and Synchronization of Chaotic Oscillations". International Journal of Bifurcation and Chaos, vol. 15, no. 8, pp. 2349–2360.

Zhou, Z. and Whiteman, 1996. "Motions of a double pendulum". Nonlinear Analysis, Theory, Methods & Applications, vol. 26, no. 7, pp. 1177–1191.

## 6 Responsibility notice

The authors are the only responsible for the printed material included in this paper.